PROCEEDINGS OF SPIE

SPIEDigitalLibrary.org/conference-proceedings-of-spie

Thermal imaging and heat islands: cross-discipline learning in optics and meteorology

Lena Heuscher, Paul W. Nugent, Joseph A. Shaw

Lena Heuscher, Paul W. Nugent, Joseph A. Shaw, "Thermal imaging and heat islands: cross-discipline learning in optics and meteorology," Proc. SPIE 11143, Fifteenth Conference on Education and Training in Optics and Photonics: ETOP 2019, 111433V (2 July 2019); doi: 10.1117/12.2524320

SPIE.

Event: Fifteenth Conference on Education and Training in Optics and Photonics: ETOP 2019, 2019, Quebec City, Quebec, Canada

Thermal imaging and heat islands: Cross-discipline learning in optics and meteorology

Lena Heuscher[a], Paul W. Nugent,[b] and Joseph A. Shaw*[b]
[a]Atmospheric Science Department, University of Alabama, 320 Sparkman Dr., Huntsville, AL USA 35899
[b]Electrical & Computer Engineering Department, Montana State University, 610 Cobleigh Hall, Bozeman, MT 59717

ABSTRACT

There are many interesting ways in which optics and meteorology intersect and provide cross-discipline learning opportunities. One example is the use of thermal imaging to illustrate the principles underlying urban heat islands (UHIs), found on scales from the mesoscale to the microscale, which give rise to increased temperatures in urban settings. The most common way of documenting such phenomena is through traditional meteorological measurements. This presentation describes the use of a thermal infrared imager to document and help explain micro-scale UHIs observed initially as a persistent difference in air temperature measured by two nearly identical weather stations separated by 2.79 km in Bozeman, Montana. Mobile meteorological measurements from a backpack-mounted weather station, carried throughout the surrounding area at different times of year and compared with the stationary campus weather station, verified the presence and scale of a micro-heat island. This also identified one such micro UHI that existed when the immediate surroundings contained man-made materials such as concrete and asphalt adjacent to natural vegetation. Thermal images from the radiometrically calibrated imager recorded the diurnal thermal signature of man-made and natural surfaces. The thermal images help to explain process that are occurring, whereas most traditional meteorological instrumentation may not provide process-based information. Time-series plots of the infrared brightness temperatures show that the man-made materials emit elevated levels of thermal radiation long after the end of direct solar heating, while natural vegetation quickly comes into thermal equilibrium with the ambient air. The combination of traditional and nontraditional instrumentation document and explain processes occurring in micro UHIs that vary rapidly in space with changing ground cover.

Keywords: Optics education, remote sensing, radiometry, thermal imaging, heat island, meteorology

1. INTRODUCTION

Optics and meteorology are branches of science with many intersecting topics, such as rainbows, halos, and other atmospheric optical phenomena that can be observed with the naked eye[1] and polarization.[2,3] Infrared radiative transfer is another subject with significant overlap between meteorology and optics, and thermal imaging provides an excellent opportunity for exploring this subject in an experimental manner that is appealing to students in both meteorology and optics. The example discussed in this paper is the use of thermal imagers to observe spatial variations of thermal radiation emitted by natural and man-made surfaces throughout a diurnal cycle, which give rise to small-scale heat islands. A heat island is a region of elevated air temperature that often arises when natural ground cover is replaced by man-made materials such as cement, asphalt, and brick.[4] While healthy vegetation continually releases its absorbed heat through transpiration, man-made surfaces absorb large amounts of solar energy and release it as long-wave infrared radiation that warms the overlying air. The difference of absorption and emission between vegetation and man-made surfaces causes temperatures to be higher around the man-made surfaces, which is known as the urban heat island effect. In general, an urban heat island (UHI) is a region of elevated air temperatures in the vicinity of a city; however, there also can be small-scale variations of the UHI on and near the urban-rural fringe. Such micro-heat islands have been found within the centers of cities[5] and also reaching into the suburbs.[6]

joseph.shaw@montana.edu; phone 1 406 994-7261; fax 1 406-994-5958; http://www.montana.edu/jshaw/

Fifteenth Conference on Education and Training in Optics and Photonics: ETOP 2019, edited by Anne-Sophie Poulin-Girard, Joseph A. Shaw, Proc. of SPIE Vol. 11143, 111433V · © 2019 SPIE, ICO, IEEE, OSA · CCC code: 0277-786X/19/$18 · doi: 10.1117/12.2524320

The UHI effect has been studied at scales from large to small, with the majority of studies addressing a UHI effect over large urban areas and a lesser number addressing smaller-scale variations. UHI's are currently being observed through remote observation using satellite and aircraft instead of the traditional ground-based observation.[7] For example, the long-standing data record from sources such as the Landsat satellites and MODIS has enabled many studies of UHI changes that accompany urban expansion in locations that include China,[8] Greece,[9] Brazil,[10] and Georgia (USA),[11] among others. The Advanced Very High Resolution Radiometer (AVHRR) was used to obtain thermal images for quantifying the magnitude of a summer heat wave in London,[12] and the Advanced Thermal and Land Applications Sensor (ATLAS) was used to study urban land cover types and thermal signatures both day and night in Alabama.[13] These studies generally explored the relationship between urban heat islands and land use and land cover change accompanying urban expansion.

While satellites excel at providing measurements over large areas and long time periods, challenges still remain with obtaining cloud-free data with sufficient spatial resolution for studying micro heat islands.[14] One approach to improving spatial resolution is to use airborne or even ground-based sensors. For example, an infrared video imaging radiometer was deployed onboard a helicopter to collect data along four main north-south routes crossing Tel Aviv, Israel and measured a UHI with finer spatial resolution than satellite images.[15] UHI effects also were quantified using mobile and stationary ground-based microwave radiometers to retrieve temperature profiles up to 600 m altitude throughout Moscow, Russia.[16]

Recent advances in methods to stabilize and calibrate low-cost, compact, uncooled thermal infrared imagers[17,18] provide an opportunity to use ground-based sensors to observe the detailed structure of micro heat islands at a much smaller scale than is practical with images from satellite or airborne platforms. In this study, a compact, uncooled, thermal infrared imager was deployed on the roof of a building on our university campus to record the diurnal variations of thermal signatures from the nearby ground, which contained a combination of vegetated and paved surfaces. The thermal image data were combined with air temperatures from an adjacent weather station to monitor the micro heat island effect on the campus. The study was extended to the region surrounding the campus through the use of a mobile, backpack-mounted weather station. This study documented spatial and temporal heat island variations on scales ranging from several km down to less than one meter.

2. EVIDENCE OF A CAMPUS HEAT ISLAND

This study began with the discovery of persistent yet temporally variable differences in air temperature measured by two nearly identical weather stations located a distance of 2.79 km from each other on the south side of Bozeman, Montana. One station operates on the roof of the engineering building at the Montana State University campus (45.667°N, 111.046°W, altitude=1.527 km), while the other operated at that time in an agricultural field (45.663°N, 111.081°W, altitude=1.495 km) used for studying technologies to detect CO_2 gas leaking from geologic carbon sequestration facilities as part of the Zero Emission Research and Technology (ZERT) program.[19,20,21]

Because of their proximity, we found it curious that these two stations measured such different air temperatures. After conducting inter-calibration tests using a third, identical temperature and humidity probe (Vaisala HMP45C) and finding less than 0.3 ºC rms calibration difference between the two stations, we realized that we must be observing real differences that were likely a result of an urban heat island. We arrived at this explanation primarily because the more urban campus location frequently experienced significantly warmer air temperatures, as is shown in Fig. 1 as a 24-hour time-series plot of the air temperatures measured by the weather stations on campus (MSU, red solid line) and in the agricultural field (ZERT, black dashed line).

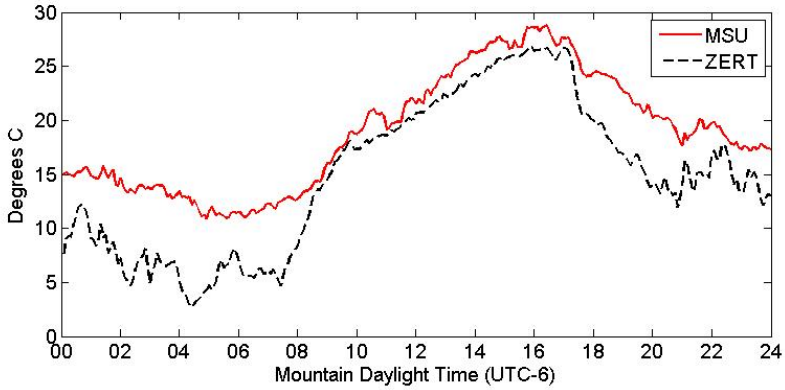

Figure 1. Time-series plot of air temperatures measured by the weather stations on campus (MSU) and at the agricultural experiment field (ZERT) on 7 Sep. 2011.

3. MOBILE METEOROLOGICAL MEASUREMENTS

After determining that the observed air-temperature differences between the MSU and ZERT weather stations were real, we used a mobile, backpack-mounted weather station to measure the spatial variation of the heat island effect continuously along a path between the two weather stations. The same mobile system was used also to explore the spatial variation of the heat island throughout the neighborhoods and along a hiking path on the other side of campus, deeper into the downtown area of Bozeman, Montana. Figure 2 shows a mobile weather station that we created with a Vaisala HMP45C humidity/temperature probe (identical to the probes used on the MSU and ZERT weather stations), a GPS receiver, and a small laptop computer. Sensor data were logged with a MATLAB program on the laptop computer.

Figure 2. Mobile backpack-mounted weather station with GPS for mapping meteorological data.

The mobile weather station was carried along a pair of paths during different times of the year to map the variation of the heat island on and near the campus. In the spring and summer of 2012, a path was followed westward across campus and across 19th Avenue, into the agricultural fields to the ZERT weather station location. Figure 3 (top) shows the path from Cobleigh Hall (A), westward across campus to W. Garfield St. (B), across S. 19th Ave. into agricultural fields, south at Wagon Wheel Road (C) to W. Lincoln Rd. (D), then westward to the ZERT weather station (E). On the return, the same path was retraced except for the final segment that followed W. Grant Rd. from (F) to the origin (Cobleigh Hall, G).

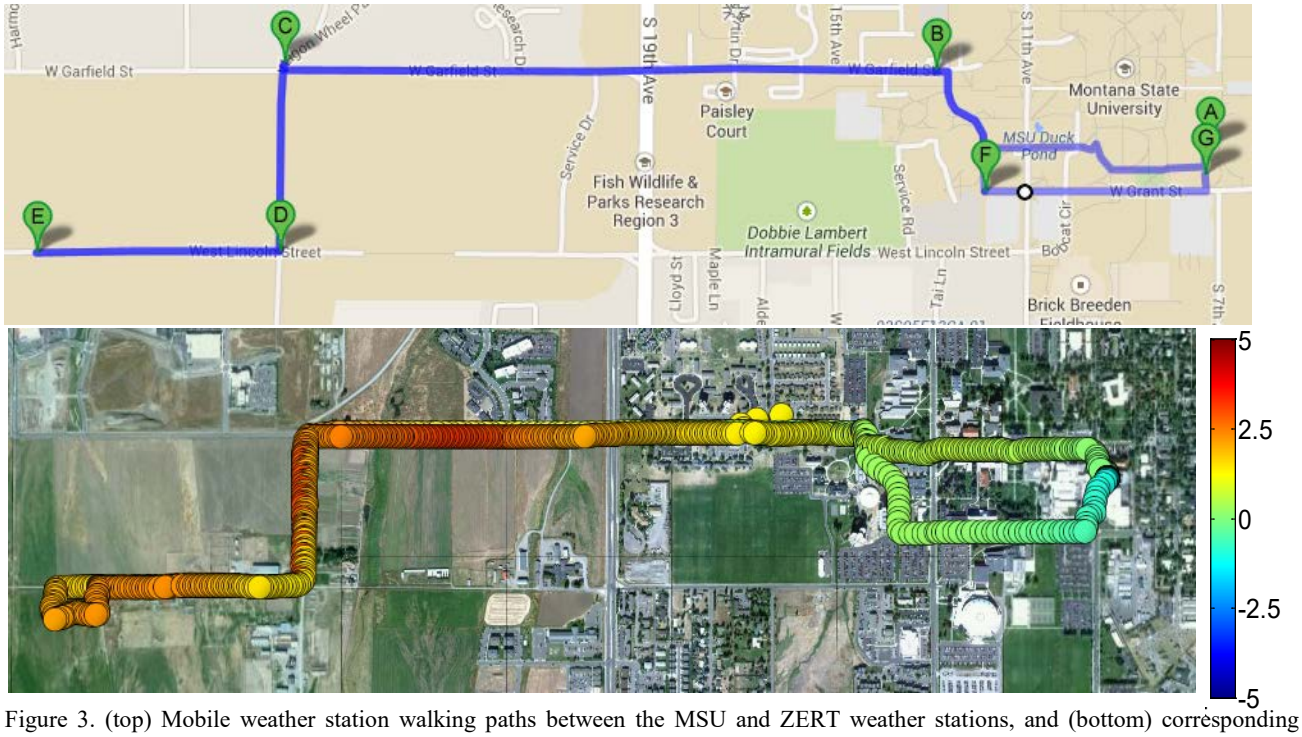

Figure 3. (top) Mobile weather station walking paths between the MSU and ZERT weather stations, and (bottom) corresponding temperature difference map (MSU-mobile, °C).

The bottom plot in Figure 3 shows air temperature differences in °C, with the mobile measurements subtracted from the stationary MSU measurements (MSU-mobile). Across the main part of campus (A-B), the mobile sensor measured air temperatures essentially equal to those measured at the stationary MSU sensor on the roof of Cobleigh Hall (A). Just west of (B), the air-temperature difference began to shift to larger positive values, indicating that the mobile sensor was measuring warmer air than the MSU sensor. The largest change occurred when the mobile sensor was carried across 19th Ave., into agricultural fields where the air temperature was approximately 2-4°C cooler than on campus (i.e., the temperature difference was positive, showing the presence of a heat island).

A different path was followed on 11 November 2012, this time heading west and north from the center of campus, as shown in Fig. 4. This path went from the North Hedges dormitory (A), through the middle of campus (A to B), northward along 8th Ave. (B to C), eastward along Main St. to the Bozeman Public Library (C to D), and then back to campus along a hiking trail (D to E) and Garfield Street (E to F). This walk was repeated in both directions (A to F and F to A) and at two different times (12:00 p.m. GMT and 2:00 a.m. GMT) to verify consistent results.

The temperature-difference map in Fig. 4 (right) shows that after a transient during the first segment (A-B), the mobile sensor measured an air temperature similar to the MSU measurements from points B to D (zero temperature difference), meaning that there was a consistent heat island up to and along Main St. because this segment was surrounded most immediately by cement sidewalks and paved streets. The temperature difference turned consistently positive as soon as the mobile sensor was carried away from Main St. and onto the hiking trail near point D, indicating that the mobile sensor measured a lower air temperature along this more vegetation-rich, unpaved trail. This illustrates the micro-meteorological scale on which the urban heat island can vary, with the air temperature along the hiking trail remaining consistently 1-2 °C cooler than on campus. Even though the hiking trail lies between paved streets, it is surrounded most immediately by natural vegetation, which leads to cooler air.

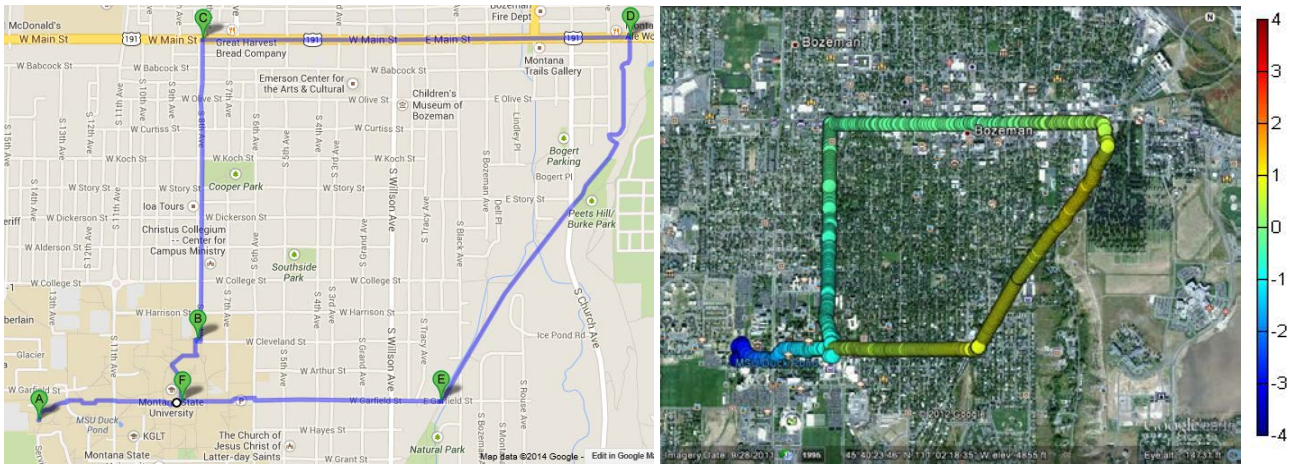

Figure 4. (left) Mobile weather station path from the MSU weather station into downtown and return along a hiking trail, and (right) corresponding temperature difference map (MSU-mobile, °C).

4. THERMAL IMAGING TO UNDERSTAND MICRO-SCALE HEAT ISLANDS

To more completely characterize the micro heat islands in the immediate vicinity of the MSU weather station, we mounted a radiometrically calibrated thermal imager on the roof of Cobleigh Hall near the stationary MSU weather station. The long-wave infrared thermal imager was a FLIR Photon 320 with 324×256 pixels, 50°×39° angular field of view, and optical bandwidth of approximately 7.5-13.5 μm. The uncooled microbolometer imager was calibrated with procedures developed at Montana State University to enable long-term outdoor deployment with stable and radiometrically accurate output.[16,17] The imager was deployed for multiple days and nights in each of three positions to obtain continuous thermal measurements (with 1-min sample period) looking west and southwest onto campus and southeast into an adjacent neighborhood. Figure 5 shows a photograph of the west view into campus (the other views had similar varieties of sidewalks, vegetation, and buildings), and Fig. 6 shows a corresponding thermal image.

Thermal images were calibrated in units of radiance [W/(m^2 sr)] and then converted to brightness temperature, or the temperature of an ideal blackbody emitting the observed radiance. In all the thermal images, the brightness temperatures were averaged over two regions, each with approximate area of 2-3 m^2: region 1 was filled by a man-made surface such as cement sidewalk or brick wall, and region 2 was filled by natural vegetation. The resulting region 1 and region 2 brightness temperatures are plotted vs. time, along with air temperature and solar irradiance measured by the MSU weather station, for 9 October 2013 (Fig. 7) and 27 October 2012 (Fig. 8). The difference in these time periods appears to be driven primarily by cloudiness, which fluctuations in the solar irradiance curves suggest was higher in the afternoon for Fig. 7 and higher in the morning for Fig. 8.

The data shown in Figs. 7 and 8 are plotted over a 24-hour period, from midnight to midnight, with noon at the center (thermal images were recorded once each minute, while the meteorological data were recorded once each 5 minutes). The top panel of Figs. 7 and 8 display brightness temperature for the two regions in the thermal images and air temperature measured at the MSU weather station; the middle panel displays the infrared (IR) brightness temperature difference between man-made and natural surfaces (region 1 – region 2); and the bottom panel displays the solar irradiance measured at the MSU weather station. The solar irradiance plots show that sunrise occurred near 0730 Mountain Daylight Time (MDT, or UTC-6 hours) and sunset occurred near 1830 MDT on both days.

A heat island effect is indicated when the temperature difference in the central panel of Figs. 7 and 8 is greater than zero, indicating that the man-made surface was radiating with a higher brightness temperature than the natural vegetation surface. In both of these figures, the brightness temperature difference was negative only during the midday hours when the Sun was directly illuminating the surfaces in regions 1 and 2. This occurred for 1000-1230 MDT in Fig. 7 and 1100-1500 MDT in Fig. 8. These differences in timing appear to be driven by cloudiness, which the solar irradiance curves suggest was higher in the afternoon for Fig. 7 and higher in the morning for Fig. 8.

Figure 5. Photograph of the west campus view from the rooftop where the thermal imager was mounted.

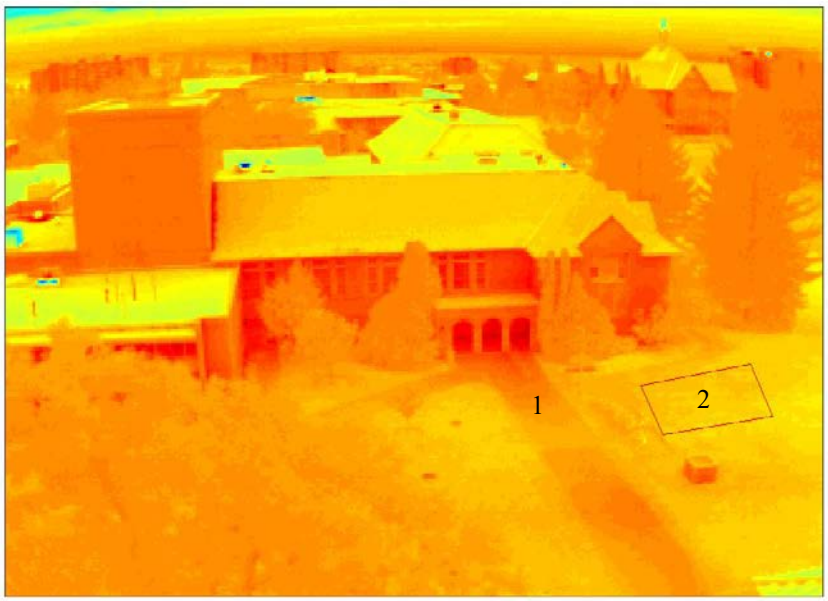

Figure 6. Thermal image looking west into the MSU campus on 9 October 2013 at 00:00 MDT (UTC-6). In this image, region 2 (vegetation) was selected in the area indicated by the box near the lower right, while region 1 (man-made material) was selected on the cement sidewalk just left of region 2.

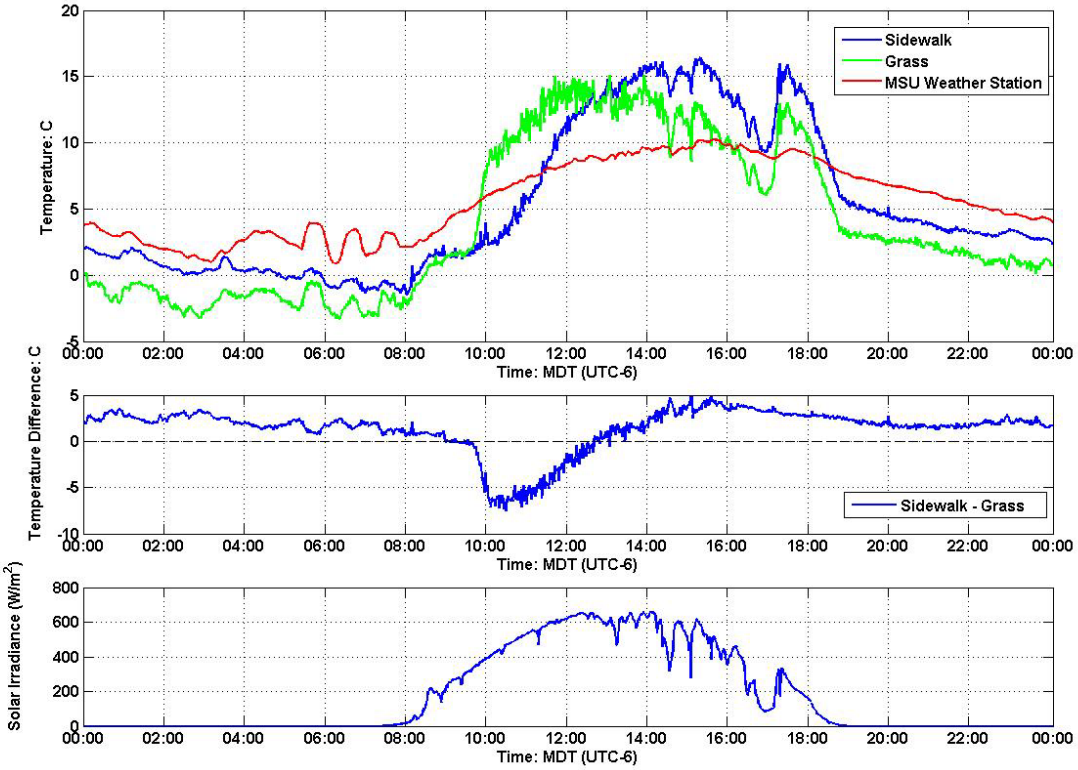

Figure 7. Time-series plots for 9 October 2013: (top) IR brightness temperatures from region 1 (man-made surface, blue curve) and region 2 (natural vegetation, green curve) in the thermal images and air temperature at the MSU weather station (red curve); (middle) difference of IR brightness temperatures for region 1 – region 2; (bottom) solar irradiance.

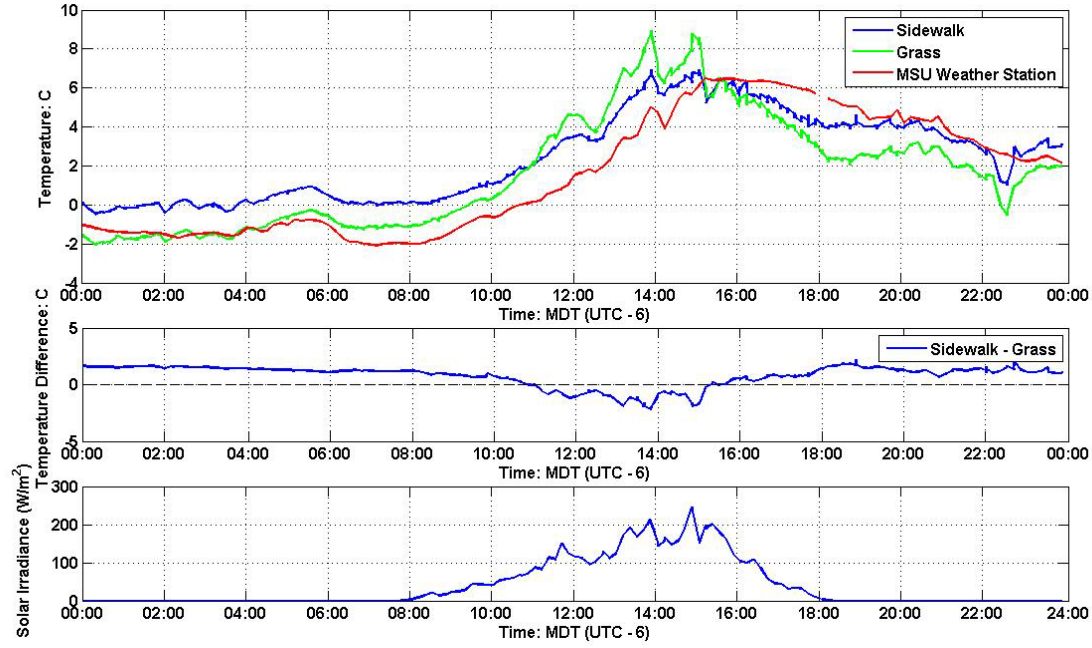

Fig. 8. Time-series plots for 27 October 2012: (top) IR brightness temperatures from region 1 (man-made surface, blue curve) and region 2 (natural vegetation, green curve) in the thermal images and air temperature at the MSU weather station (COB, red curve); (middle) difference of IR brightness temperatures for region 1 – region 2; (bottom) solar irradiance.

Careful examination of Figs. 7 and 8 shows evidence of numerous rapid changes in the thermal radiation that are directly correlated with the temperature and solar irradiance plots. For example, at approximately 1500 MDT in Fig. 8, a spike in solar irradiance, which appears to have been caused by the sun emerging from behind clouds, occurred with a corresponding trend in air temperature and IR brightness temperature difference. In general, whenever the regions of interest were not directly illuminated by sunlight, the negative brightness temperature difference shows that the man-made surfaces were emitting more thermal radiation than the vegetation. This routinely led to warmer air temperatures in the vicinity of the man-made surfaces, which indicates the physical source of a micro heat island. Man-made surfaces produced a significant heat island effect in all three directions in which thermal images were recorded – both on campus and in the adjacent neighborhood. Similar patterns occurred throughout the study period. As an aside, it is interesting to note the evidence of atmospheric gravity waves in the temperature graphs of Fig. 7 (~05:00 – 08:00 MDT), with amplitude of approximately 3 °C and period of about one hour, which give rise to a 1°C fluctuation in the IR brightness temperature difference (and hence the local micro heat island).

5. CONCLUSION

Urban heat islands are widely recognized and studied, but this study using a stationary, accurately calibrated thermal imager has illustrated changes in the thermal radiation from man-made and naturally vegetated surfaces on small spatial and temporal scales that drive the dynamics of micro heat islands. This method was coupled with a combination of stationary and mobile meteorological sensors to map an urban heat island in Bozeman, Montana, USA that appeared and disappeared as the mobile sensor was transported through regions immediately surrounded by man-made or vegetated surfaces. This approach can help explain and measure the dynamics of the micro-scale urban heat island effect on scales that cannot be studied practically with airborne or satellite imagery. The study presented here illustrates how thermal imagers, which are becoming increasingly available at lower cost, can be used in teaching principles related to thermal radiation, radiative transfer in the atmosphere-Earth system, meteorology, and of course optical imaging.

Acknowledgment

This material is based upon work supported by the Department of Energy under award number DE-FE0000397. This report was prepared as an account of work sponsored by an agency of the United States Government. Neither the United States Government nor any agency thereof, nor any of their employees, makes any warranty, express or implied, or assumes any legal liability or responsibility for the accuracy, completeness, or usefulness of any information, apparatus, product, or process disclosed, or represents that its use would not infringe privately owned rights. Reference herein to any specific commercial product, process, or service by trade name, trademark, manufacturer, or otherwise does not necessarily constitute or imply its endorsement, recommendation, or favoring by the United States Government or any agency thereof. The views and opinions of authors expressed herein do not necessarily state or reflect those of the United States Government or any agency thereof.

REFERENCES

[1] Shaw, J. A., [Optics in the air: Observing optical phenomena through airplane windows], SPIE, Bellingham, WA (2017).
[2] Tyo, J. S., D. L. Goldstein, D. B. Chenault, and J. A. Shaw, "Review of passive imaging polarimetry for remote sensing applications," Appl. Opt. 45(22), 5453-5469 (2006).
[3] Shaw, J. A., "Infrared polarization in the natural Earth environment," Proc. SPIE 4819, 123-139 (2002).
[4] American Meteorological Society, [Glossary of Meteorology], "urban heat island," http://glossary.ametsoc.org/wiki/urban_heat_island.
[5] Aniello, C., K. Morgan, A. Busbey, and L. Newland, "Mapping micro-urban heat islands using LANDSAT TM and a GIS," Computers & Geosciences 21(8), 965-969 (1995).
[6] Xie, H., N.-B. Chang, D. Prado, and A. Daranpob, "Assessing the long-term urban heat island in San Antonio, Texas based on moderate resolution imaging spectroradiometer/Aqua data," J. Applied Rem. Sens. 4(1), 043508 (2010).
[7] Voogt, J. A., T. R Oke, "Thermal remote sensing of urban climates," Remote Sens. Env. 86(3), 370-384 (2003).

[8] Zhang, H., Z.-F. Qi, X.-Y. Ye, Y.-B. Cai, W.-C. Ma, and M.-N. Chen, "Analysis of land use/land cover change, population shift, and their effects on spatiotemporal patterns of urban heat islands in metropolitan Shanghai, China," Applied Geography 44(121), 0143-6228 (2013).
[9] Stathopoulou, M. and C. Cartalis, "Daytime urban heat islands from Landsat ETM+ and Corine land cover data: An application to major cities in Greece," Solar Energy 81(3), 358-368 (2007).
[10] Apolônio Callejas, I. .J., A. S. de Oliveira, F. M. de Moura Santos, L. C. Durante, M. C. de J. A. Nogueira, and P. Zeilhofer, "Relationship between land use/cover and surface temperatures in the urban agglomeration of Cuiabá-Várzea Grande, Central Brazil," J. Appl. Rem. Sens. 5(1), 053569 (2011).
[11] Lo, C. P. and D. A. Quattrochi, "Land-Use and Land-Cover Change, Urban Heat Island Phenomenon, and Health Implications," Photogrammetric Engineering & Remote Sensing 69(9), 1053-1063 (2003).
[12] Holderness, T., S. Barr, R. Dawson, and J. Hall, "An evaluation of thermal Earth observation for characterizing urban heatwave event dynamics using the urban heat island intensity metric," International J. Remote Sens. 34(3), 864-884, (2012).
[13] Lo, C. P., D. A. Quattrochi, and J. C. Luvall, "Application of high-resolution thermal infrared remote sensing and GIS to assess the urban heat island effect," International J. Remote Sens. 18(2), 287-304 (1997).
[14] Chudnovsky, A., E. Ben-Dor, and H. Saaroni, "Diurnal thermal behavior of selected urban objects using remote sensing measurements," Energy and buildings 36(11), 1063-1074, (2004).
[15] Ben-Dor, E. and H. Saaroni, "Airborne video thermal radiometry as a tool for monitoring microscale structures of the urban heat island," Int. J. Remote Sens. 18(14), 3039-3053 (1997).
[16] Kadygrov, E., M. Khaikine, I. Kuznetsova, and E. Miller, "Investigations of urban heat island on the basis of stationary and mobile microwave systems for remote measurements of atmospheric temperature profile," Proc. SPIE 5832, 502-513 (2005).
[17] Nugent, P. W., J. A. Shaw, and N. J. Pust, "Correcting for focal-plane-array temperature dependence in microbolometer infrared cameras lacking thermal stabilization," Opt. Eng. *52*(6), 061304 (2013).
[18] Nugent, P. W. and J. A. Shaw, "Calibration of uncooled LWIR microbolometer imagers to enable long-term field deployment," Proc. SPIE 9071, 90710V (2014).
[19] J. A. Hogan, J. A. Shaw, R. L. Lawrence, J. L. Lewicki, L. M. Dobeck, L. H. Spangler, "Detection of leaking CO_2 gas with vegetation reflectances measured by a low-cost multispectral imager," *J. Selected Topics Appl. Earth Obs. Remote Sens*. **5**(3), 699-706 (2012) [doi:10.1109/JSTARS.2012.2202880].
[20] J. E. Johnson, J. A. Shaw, R. L. Lawrence, P. W. Nugent, L. M. Dobeck, and L. H. Spangler, "Long-wave infrared imaging of vegetation for detecting leaking CO_2 gas," *J. Appl. Rem. Sens.* **6**(1), 063612 (2012) [doi: 10.1117/1.JRS.6.063612].
[21] J. E. Johnson, J. A. Shaw, R. L. Lawrence, P. W. Nugent, J. A. Hogan, L. M. Dobeck, and L. H. Spangler, "Comparison of long-wave infrared imaging and visible/near-infrared imaging of vegetation for detecting leaking CO_2 Gas," *J. Selected Topics Appl. Earth Obs. Remote Sens*. (2014) [doi: 10.1109/JSTARS.2013.2295760].